

# Structural Modeling and Design Considerations for Double-Layer Shoring Systems

Jui-Lin Peng<sup>1</sup>

**Abstract:** This paper presents structural modeling and design considerations for a double-layer shoring system made of wood posts based on analytical derivation, numerical computation, and the LeMessurier formula. Simplified two-dimensional models of double-layer shoring systems are developed. The analysis shows that system critical loads do not increase with the addition of individual pinned-ended shores, i.e., leaning columns, in the system during construction. If these individual pinned-ended shores are widely used, more cases of falsework failure may occur. The effects of lengths of horizontal stringers and vertical shores, stiffnesses of stringers, and positions of strong shores are investigated in the paper. The reinforcement by addition of bracing to the shoring systems can improve the system buckling strength. The study concludes that appropriately fastening a group of pinned-ended shores with horizontal bracings, i.e., strong shores, can increase the load-carrying capacity of a double-layer shoring system.

**DOI:** 10.1061/(ASCE)0733-9364(2004)130:3(368)

**CE Database subject headings:** Critical load; Shoring; Falsework; Columns; Structural models.

## Introduction

Falsework is widely used to support construction loads, which consists of fresh concrete, steel, formwork, workers, etc., before sufficient concrete strength is developed during construction. An elevated slab forming in Fig. 1 shows a double-layer shoring system. The length of the vertical shores is not capable of filling in the headroom between the soffit formwork and the slab on ground due to the shore length limitation manufactured by factories. A double-layer shoring system is considered to solve the supporting problem in falsework. In Taiwan, most reinforced concrete buildings with headroom 4–7 m (13.1–23 ft) are constructed by double-layer shoring systems as falsework (Fig. 1). Two types of shores used in double-layer systems are usually adopted: the wood post shore and the telescopic prop (see Fig. 2). Owing to the lack of a theoretical base for safety and design specifications for the falsework, the shoring system has a threat of collapse during construction. Based on the reports of “Investigations of construction accidents” (Council 1997), the deficiency of falsework strength usually results in the collapse of double-layer shoring systems. A collapse case of a double-layer shoring falsework is shown in Fig. 3. One construction worker was killed and eight others were injured in this construction accident.

For reinforced concrete buildings with headroom higher than 7 m (23 ft), research on the falsework of scaffold shoring used in construction was conducted (Peng et al. 1996a,b, 1997). In multistory concrete buildings, much research (Mosallam and Chen 1990; El-Shahhat et al. 1994) has been undertaken concerning the

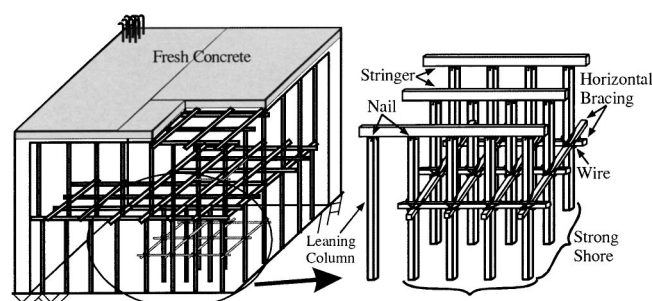
use of shores and reshores. The headroom of each story in these multistory buildings is less than 4 m (13.1 ft). Research on system strength in one-layer shoring systems was conducted by Peng (2002). However, little research was carried out in the area of double-layer shoring systems used in construction.

The telescopic prop is not investigated in this research since the “overlap joint” is another key point to the strength. As shown in Fig. 2, the length of the upper post of a telescopic prop is constant and is equal to  $h_1$  plus  $h_2$ . In practice, the overlap length between the upper and lower posts at the joint,  $h_2$ , needs to be adjusted based on the headroom change of the building. The length of the overlap affects the strength of the telescopic prop. The telescopic props are not discussed in this paper.

Fig. 1 presents the terminology used to discuss the double-layer shoring system. In this study, the strong shore is defined as the vertical shores with horizontal bracings, fastened appropriately with a wire. Individual shores connected to horizontal stringers with nails are defined as leaning columns in the analysis.

## Material Properties

The wood post is made of Kapur. The material properties of wood posts measured in the material testing laboratory of Yunlin Uni-



**Fig. 1.** Setup and terminology of double-layer shoring system during construction

<sup>1</sup>Associate Professor, Dept. of Construction Engineering, Yunlin Univ. of Science and Technology, Taiwan, R.O.C.

Note. Discussion open until November 1, 2004. Separate discussions must be submitted for individual papers. To extend the closing date by one month, a written request must be filed with the ASCE Managing Editor. The manuscript for this paper was submitted for review and possible publication on June 5, 2001; approved on December 16, 2002. This paper is part of the *Journal of Construction Engineering and Management*, Vol. 130, No. 3, June 1, 2004. ©ASCE, ISSN 0733-9364/2004/3-368-377/\$18.00.

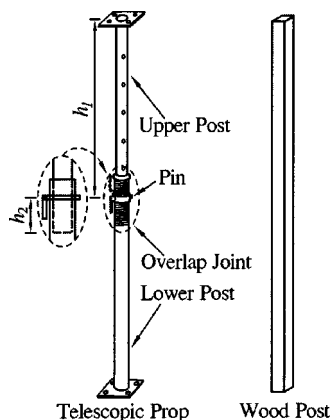


Fig. 2. Individual telescopic prop and wood post

versity of Science and Technology are listed as follows: (1) Young's modulus of elasticity = 12.47 GPa (1809 ksi); (2) rectangular cross section = 5.6295 cm × 5.882 cm (2.2 in. × 2.32 in.); (3) cross-sectional area = 33.11 cm<sup>2</sup> (5.13 in.<sup>2</sup>); and (4) second moment of area  $I_y = 87.45 \text{ cm}^4$  (2.10 in.<sup>4</sup>) and  $I_z = 95.47 \text{ cm}^4$  (2.29 in.<sup>4</sup>).

## Analysis Models

### Formulation

The analysis presented here is based on a second-order elastic analysis (i.e., geometric nonlinear/material linear analysis). An equivalent lateral notional force of 0.1–0.5% of total vertical loads is used to simulate the initial imperfection of the double-layer shoring system. The computer program *GMNAF* developed by Chan (Chan and Zhou 1994) is used in the paper. This program adopts a second-order elastic analysis using the pointwise equilibrating polynomial element. Compatibility at end nodes and the equilibrium for moment and shear at midspan are maintained, which overcomes the error associated with conventional displacement based on finite element. The present element is fifth order and different from the conventional cubic finite element which is only suitable for linear or moderate nonlinear problems.



Fig. 3. Collapse of double-layer shoring system made of wood posts during construction in Keelung, Taiwan, R.O.C.

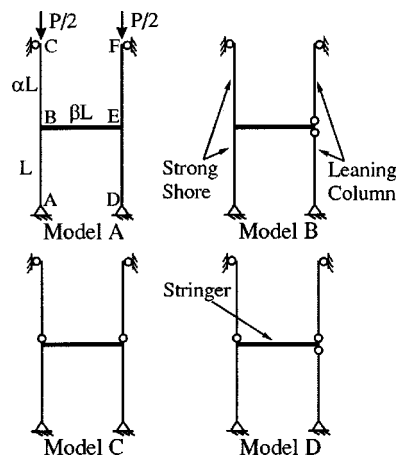


Fig. 4. Terminology and basic analysis models of 1-bay system

### Structural Model

Fig. 4 shows four basic models, i.e., models A, B, C, and D. These four models differ in the numbers and positions of strong shores. For model A in Fig. 4, all four shores are strong shores, which are composed of vertical shores and horizontal bracings combined as a closed-form system on construction sites (see Fig. 1). In model B, the shores on the left are strong shores and those on the right are "leaning columns," which are pinned at both ends of the shoring.

The definition of "leaning columns" was given by LeMesurier (1977). As shown in Fig. 5, two portal frames have the same dimensions but different connection stiffness at the top of the right column. The right column CD in Fig. 5.2 cannot resist any sideways motion since it is pinned at both ends. This pinned-ended column is defined as a leaning column and its effect changes the effective length factor  $K$  of the left column AB in the frame from 2.0 in Fig. 5.1 to 2.695 in Fig. 5.2. Thus the strength of the portal frame reduces by half [ $1.8 = (2.695/2)^2$ ] for the leaning column effect.

In the analysis, model A without leaning columns in Fig. 4 is the upper bound solution of the shoring system and model D with three leaning columns is the lower bound result. The buckling loads of models B and C with two leaning columns are apparently between these two solution bounds. As seen in Fig. 4,  $\alpha$  is the ratio of the length of the top column to that of the bottom column. Similarly,  $\beta$  is the ratio of the lengths of the horizontal stringer to the bottom column. Fig. 6 shows different configurations of two bays. The definitions of  $\alpha$ ,  $\beta$ , and  $L$  are the same as in Fig. 4.  $E_h$  and  $E_v$  = elastic moduli of horizontal members and vertical

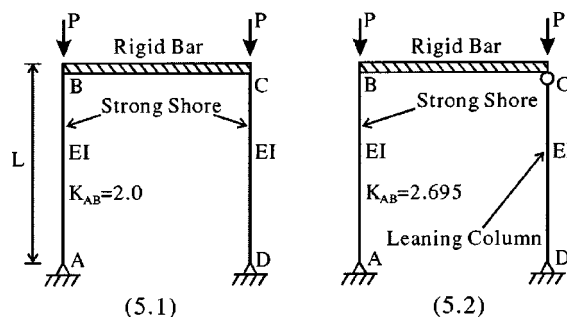


Fig. 5. Definition of leaning column and strong shore in portal frame

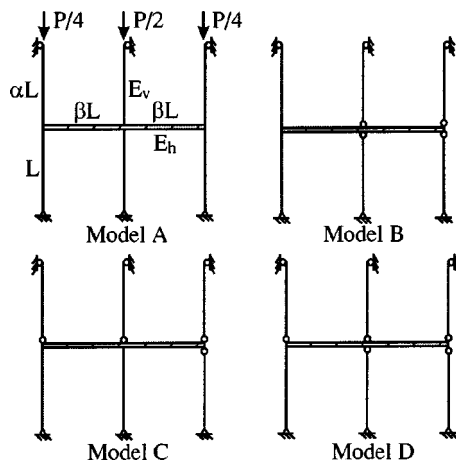


Fig. 6. Analysis models of 2-bay system

shores. These two basic models for 1- and 2-bay shoring systems are used in the following analysis.

### Loading Model

Uniform load due to the weight of fresh concrete placed on the formwork is considered. Based on the locations of the shores, the loading in the analysis is expressed in Fig. 7. The loading applied on the edge shoring of the system is half of the load acting on the middle shoring as shown in Fig. 7. The definitions of  $\alpha$ ,  $\beta$ , and  $L$  are the same as in Figs. 4 and 6.

## Analysis, Results and Discussion

### Leaning Column Effect to Two-Dimensional and Three-Dimensional Shoring Systems

Both two-dimensional (2D) and three-dimensional (3D) models are analyzed in this section. A simplified 2D analysis will be used to model the complicated 3D problem in the following sections if the results of these two analyses are similar. For easy comparison of the test results, it is first assumed that the stiffness of horizontal stringers is equal to that of vertical shores.

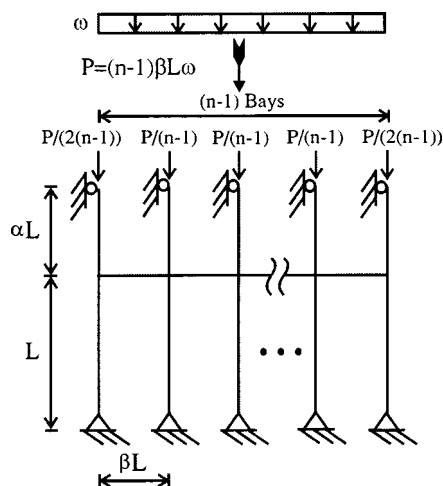


Fig. 7. Loading models of system

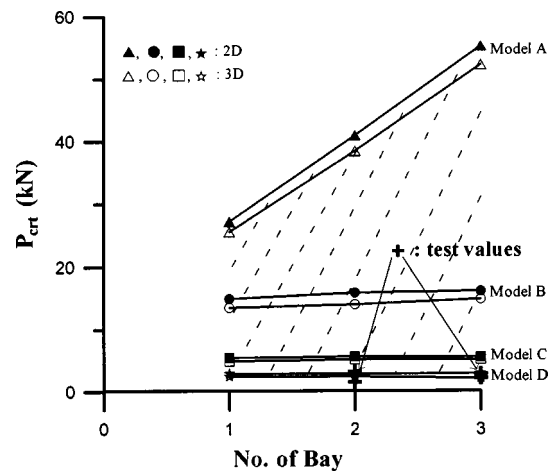


Fig. 8. Critical loads of double-layer systems with leaning column effect [ $E_v = E_h = 12.47$  GPa (1,809 ksi),  $L = 300$  cm (9.8 ft),  $\alpha = 0.6$ ,  $\beta = 0.2$ ]

Fig. 8 presents an analysis result of the effect of leaning columns on double-layer shoring systems. As shown in Fig. 8, the solid symbols represent the analysis results of the 2D model and the hollow symbols are for the 3D model. The experimental test results of 2-bay and 3-bay shoring systems are listed with the symbol “+” in the same figure. The 1-bay and 2-bay systems are shown in Figs. 4 and 6. Similarly, the 3-bay system on the  $x$  axis in Fig. 8 is an extension of the 1-bay and 2-bay models.

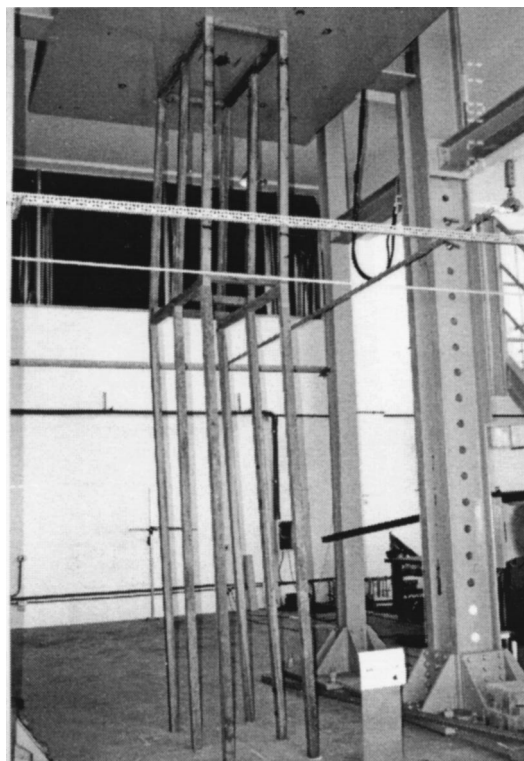
All shores are strong shores in model A, which can be considered as the upper bound failure load of the shoring systems. Leaning columns are present in models B, C, and D. All setups of leaning columns defined in these three models are actually used on a construction site in Taiwan. As shown in Fig. 1, if shores tied with horizontal bracings are formed in a closed pattern or the end nodes of an individual shore are suitably fixed, these shores are considered as an equivalent strong shore; otherwise, they are regarded as leaning columns.

In Fig. 8, the system critical loads of model A increase linearly with the bay numbers while critical loads of models B, C, and D are constant regardless of the number of bays in the systems. For model A, two additional strong shores are installed for every addition of a bay. This arrangement leads to the system critical load to increase linearly. In contrast, models B, C, and D possess two more leaning columns for every addition of one bay and their buckling loads are significantly less than model A. The horizontal force on the stringer induced by the leaning column does not increase the system critical load.

The system critical load of model B is larger than model C despite the fact that they both have two strong shores. According to relativity theories of leaning column effect (LeMessurier 1977), more leaning columns lead to a smaller critical load in a shoring system. Further, a shorter leaning column will create a larger horizontal force on columns during loading. Since the length of the bottom shores (300 cm) (9.8 ft) in the systems is larger than top shores (180 cm) (5.9 ft), the number of shorter leaning columns of model C is larger than model B. Therefore the system critical load of model C is smaller than model B, as shown in Fig. 8.

In Fig. 8, the critical loads of model B are about three times those of model C for different numbers of bays. This indicates





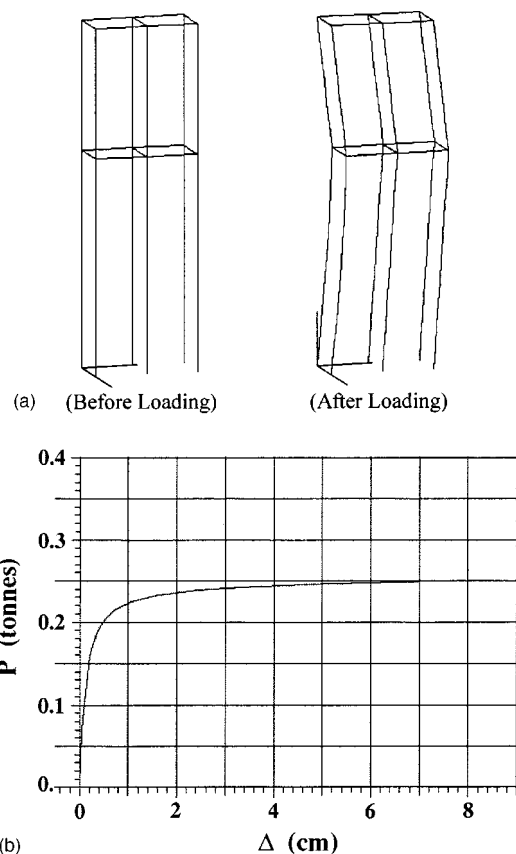
**Fig. 9.** Test of a 2-bay double-layer shoring system made of wood posts

that model B is superior to model C in terms of system strength. As seen in Figs. 4 and 6, the big difference between models B and C is the positions of strong shores. Two strong shores are set up on the same vertical line in model B. This provides construction practitioners valuable hints on installation of strong shores in this specific double-layer shoring system.

In summary, the system critical loads are determined by the numbers of strong shores in the system. More strong shores lead to a bigger system critical load. On the other hand, increasing the number of leaning columns does not improve the system critical load. This indicates that leaning columns make no contribution to the critical loads of the shoring systems.

Fig. 9 shows a 2-bay shoring system in the test. The dimensions of the computer models are the same as the tested specimen. The length of bottom shores is 300 cm (9.8 ft), and the length of the upper shores is 180 cm (5.9 ft) ( $\alpha=0.6$ ), with the length of stringers 60 cm (2 ft) ( $\beta=0.2$ ). The average critical load is 2,388 N (537 lb) for two tested 2-bay shoring systems and 2,525 N (568 lb) for another two 3-bay shoring systems (see Figs. 8 and 9) (Peng et al. 1998). The experimental loads were noted to be very low compared with our expectation in practice.

As shown in Fig. 9, this test setup was based on the worst configuration with leaning columns on construction site which represented the lower failure bound of the systems. In Fig. 8, the test data of double-layer shoring systems show a similar trend to model D. Thus model D can be used to simulate the worst situation of a double-layer shoring system. In addition, Fig. 8 shows the strength distribution between upper bound (model A) and lower bound (model D) expressed by the area with dotted slant lines. The real system critical loads of double-layer shoring systems will be located in the dotted-line area based on the number of strong shores and leaning columns in the actual shoring systems on site. More strong shores in the shoring system make the



**Fig. 10.** (a) Deformed shape of 2-bay system for model D before and after loading and (b)  $P$ - $\Delta$  curve of 2-bay system for model D in 3D analysis (1 t=9.807 kN)

real system critical loads approach the curve for model A. On the other hand, fewer strong shores make the critical loads approach the curve of model D.

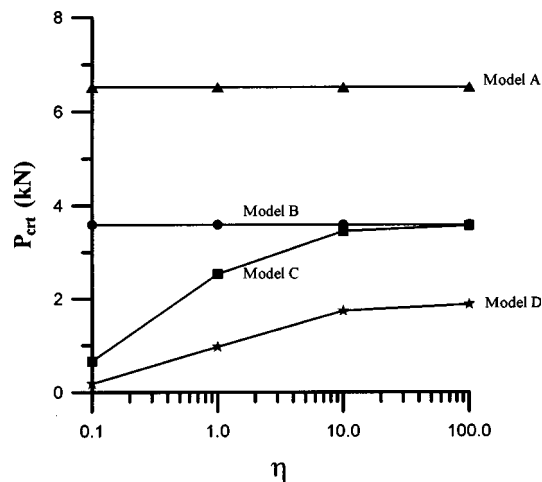
Additionally, Fig. 8 shows the analysis results of 2D and 3D models. While their results are similar, the input preparation and analysis for the 3D model are more time-consuming and tedious than the 2D model. In the present study, the 2D model is used to substitute for the 3D for efficiency in analysis.

Fig. 10(a) illustrates the deformation of the shoring system for model D before and after loading. The maximum horizontal displacement can be found at the stringer. This phenomenon conforms closely to the failure of shoring systems in tests. Fig. 10(b) shows the load-deflection curve ( $P$ - $\Delta$  curve) of model D. Since the second-order elastic analysis is used in this paper, the asymptote of the load versus deflection curve will be taken as the system critical load.

### Stiffness of Horizontal Stringers

The load-carrying capacities of shoring systems can be calculated based on various stiffness of horizontal stringers. For simplicity, a 1-bay model is first used (see Fig. 4). Both top and bottom shores have the same height of 300 cm (9.8 ft). The stiffness ratio  $\eta$   $[=(E_{\text{stringer}}I/L)/(E_{\text{shore}}I/L)]$ , defined as the stiffness ratio of horizontal stringers to vertical shores, varies from 0.1 to 100.

Fig. 11 illustrates how the system critical load varies with the stiffness of stringers. As shown in Fig. 11, when the stringer stiffness increases, the system critical loads of models A and B do not vary. This is because the double-layer shoring system is sym-

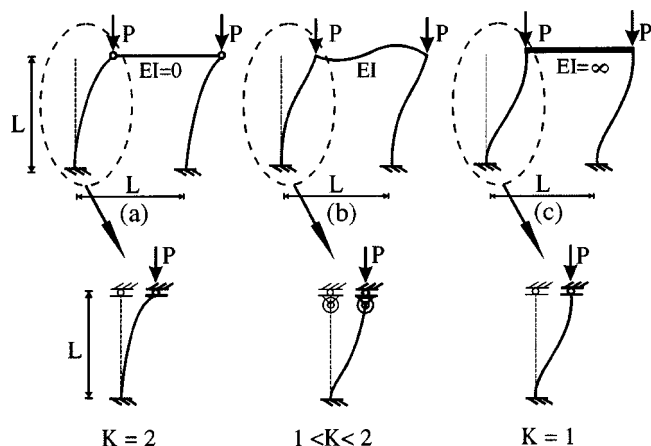


**Fig. 11.** Critical loads of double-layer shoring systems with various stiffness of stringers ( $\alpha = 1$ ,  $\beta = 1$ )

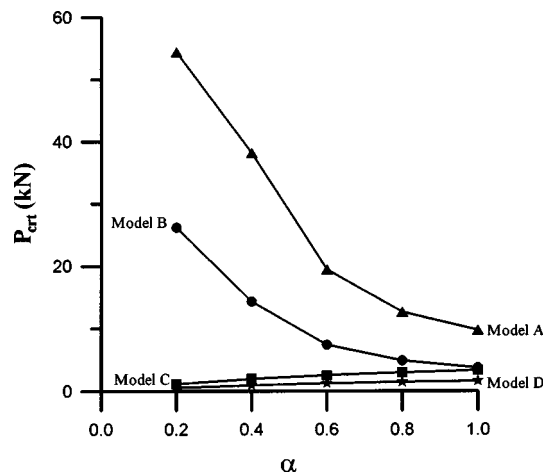
metrical about the horizontal stringer. The horizontal stringer can be regarded as an undeformed member when loading is applied to the system. Thus the system critical loads are unaffected by the increase of stringer stiffness.

Referring to models C and D in Fig. 4, both systems are unsymmetrical about the horizontal stringer. As shown in Fig. 11, both system critical loads increase with the stringer stiffness. When the stringer stiffness increases, this horizontal stringer will not easily deform during and after loading. Thus the stringer can provide extra stiffness to the load-carrying capacity of the shoring system.

Fig. 12 shows how the stiffness of a horizontal stringer influences the load-carrying capacity of an unbraced portal frame. The effective length factor  $K$  is used to measure the load-carrying capacity of the system. Fig. 12(a) shows a very soft horizontal stringer with zero  $EI$ . The left-hand column of the portal frame can be simplified as an individual column with a top hinge bound at the stringer. The  $K$  value of this column is 2.0. Fig. 12(c) presents a very rigid horizontal stringer of which the  $EI$  is infinite. The left-hand column of the portal frame can be considered as an individual column with  $K = 1.0$ . Fig. 12(b) illustrates the stringer stiffness from 0 to  $\infty$ . An individual column with a spiral spring at the top can model the stiffness induced from the stringer.  $K$  for



**Fig. 12.** Deformed shapes of simplified analysis models



**Fig. 13.** Critical loads of double-layer shoring systems with different shoring lengths ( $\beta = 0.2$ )

this specific column is between 1 and 2. Thus the system critical load of case (b) lies between case (a) and case (c).

The model of case (b) in Fig. 12 shows that the critical loads of unsymmetrical models C and D in Fig. 11 increase with stringer stiffness. Cases (a) and (c) in Fig. 12 illustrate the effect of the extreme change of stringer stiffness on the system critical loads. For models C and D, case (a) explains the values on the left range of the curves and case (c) illustrates the values on the right range of the curves in Fig. 11.

### Varied Lengths of Vertical Shores

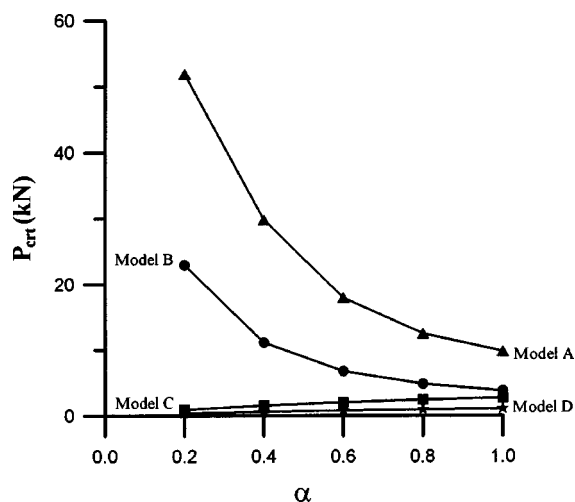
In the analysis in this section, the length of the top shore is changed and the length of the bottom shore is kept constant at 300 cm (9.8 ft). The height of the top shore is defined as  $\alpha L$ , where  $\alpha$  = ratio of the top shore length to the bottom shore length. The ratio  $\alpha$  is always less than 1. This is due to the fact that the top shore length is always less than the bottom shore length on an actual construction site. In addition, the elastic modulus of horizontal stringer and vertical shore is assumed to be identical.

Two conditions are analyzed, i.e.,  $\beta = 0.2$  and  $\beta = 1.0$ , where  $\beta$  = ratio of the lengths of the horizontal stringer to the bottom column. On a construction site, the spacing between shores varied. This is because shores need to be used in different locations such as the bottom of slabs or beams in construction. The spacing between shores under slabs and beams are always different. Additionally, the spacing needs to be adjusted in order to support different construction loads. For simplicity, only a 1-bay model is considered in the analysis.

### Stringer Length of 60 cm ( $\beta = 0.2$ )

Fig. 13 reveals how critical loads vary with different lengths of top shores when  $\beta = 0.2$ . Four models A, B, C, and D are analyzed (see Fig. 4). The length on spacing of horizontal stringer of 60 cm (2 ft) is used in the full-scale tests (see Fig. 9). As shown in Fig. 13, the system critical loads of models A and B decrease and those of models C and D slightly increase with  $\alpha$ .

For a specific value of  $\alpha$ , the shorter the leaning column, the smaller the system critical load. This is because the shorter leaning column induces a higher lateral force in the system. For example, if  $\alpha$  is 0.6, the system critical load  $P_{cr}$  of model B is 7,404 N (1,664 lb), which is larger than model C of 2,560 N (575 lb). This is because the leaning columns in model C are shorter than



**Fig. 14.** Critical loads of double-layer shoring systems with different shoring lengths ( $\beta = 1.0$ )

those in model B, though the leaning columns are placed at different positions. Thus the system critical load of model C is smaller than model B. This implies that workers need to install the leaning columns in positions with longer lengths, such as the bottom story in this section. This arrangement will help to increase system strength. The finding is useful for site foremen and engineers in checking and design falsework in construction.

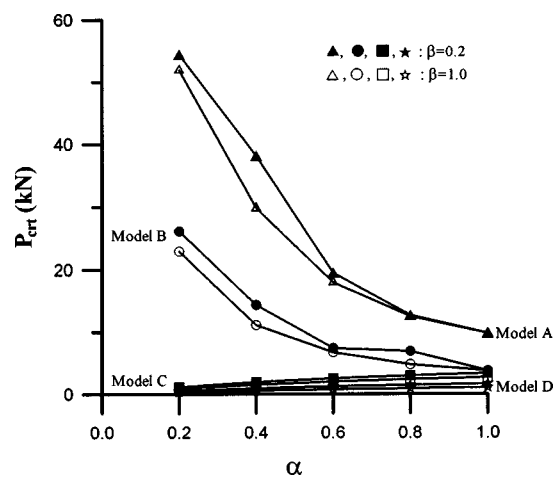
As shown in Fig. 13, since models C and D have the same number of shorter leaning columns on the top story, their system critical loads are similar although model D has one more longer leaning column in the bottom story. Besides, model C shows that a shorter leaning column reduces the system critical load. Models B and C have very similar system critical loads when the length of the top and bottom shores are equal (i.e.,  $\alpha = 1$ ). Except for the different positions of leaning columns, models B and C have the same number of leaning columns.

All shores in model A are strong shores. This makes model A have a higher load-carrying capacity than other models. Thus model A can be regarded as an upper bound of these four analysis models. On the contrary, model D can be considered as a lower bound of these models since it has only one strong shore in the system. The practical strength of a 1-bay double-layer shoring system on a construction site should be located between these two curves.

#### Stringer Length of 300 cm ( $\beta = 1.0$ )

For practical reasons mentioned above, the stringer length sometimes needs to be changed in construction. For an extreme comparison with the shorter stringer, the following analysis uses 300 cm (9.8 ft) (i.e.,  $\beta = 1.0$ ) as the length of the stringer. Fig. 14 shows how critical loads vary when  $\beta = 1.0$ . The patterns of the four curves are quite similar to those in Fig. 13.

Fig. 15 shows the values of the models of  $\beta = 1.0$  and  $\beta = 0.2$ . In the figure, the solid symbols ( $\blacktriangle$ ,  $\bullet$ ,  $\blacksquare$ ,  $\star$ ) represent the values from the model of  $\beta = 0.2$  and the hollow symbols are for the model of  $\beta = 1.0$ . As shown in Fig. 15, the values of the model of  $\beta = 1.0$  are always smaller than the model of  $\beta = 0.2$ . This indicates that an increase of stringer length marginally reduces the strength of the double-layer shoring system.

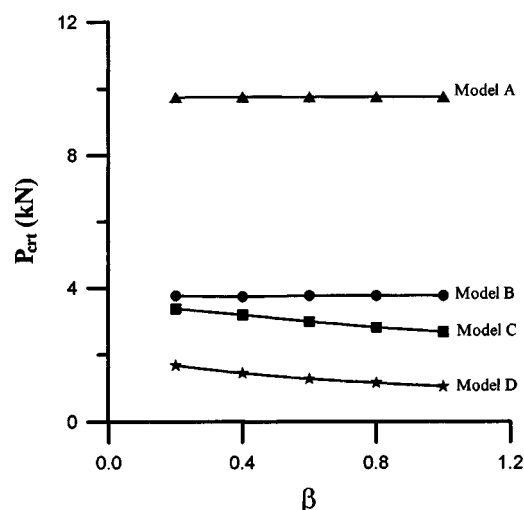


**Fig. 15.** Comparison of system critical loads between models of  $\beta = 0.2$  and  $\beta = 1.0$

#### Varied Lengths of Horizontal Stringers

In the analysis of this section, the system strengths of varied lengths of stringers with a constant of shoring height 300 cm (9.8 ft) (i.e.,  $\alpha = 1.0$ ) are considered. The elastic modulus of horizontal stringers  $E_h$  is equal to the vertical shoring on the top and bottom  $E_v$ . Young's modulus of elasticity of 12.47 GPa (1,809 ksi) is used in both models. The length ratio  $\beta$  is the ratio of the lengths of the horizontal stringer to the bottom column.

Fig. 16 shows the variation of critical loads with the different lengths of stringers. In the figure, the curves derived from models A and B are constant. This is because the top and bottom shores are setup symmetrically to the horizontal stringer. However, the curves derived from models C and D decrease slightly and linearly. This is because the shorter horizontal stringer provides higher end spiral stiffness at the end of the shoring. The length of the horizontal stringer slightly increases, so the end stiffness is not greatly reduced. This is the reason why the curve does not decrease sharply for models C and D.



**Fig. 16.** Critical loads of double-layer shoring systems with different stringer lengths ( $E_h = E_v$ )

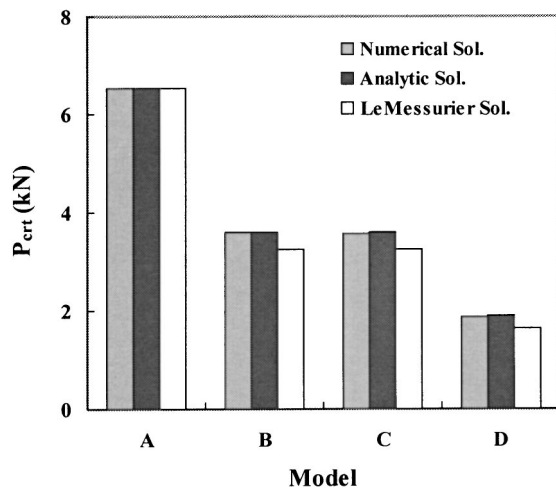


Fig. 17. Comparison of system critical loads among numerical, analysis, and LeMessurier formula solutions

### Numerical, Analytic and LeMessurier's Solutions

#### Solution Comparison of 1-Bay System

Numerical, analytic, and LeMessurier's methods (1997) are used to analyze the strengths of double-layer shoring systems. The analytic solution is used to verify the numerical solution with the aid of computers. The LeMessurier formula is used to substitute for the complicated computer calculation in shoring design. For simplicity, a 1-bay double-shoring system (see Fig. 4) with a shoring height of 300 cm (9.8 ft) is considered, and the stiffness ratio of horizontal stringer to vertical shores is 100.

For clarity, the solutions derived from the computer, analytic, and LeMessurier's calculations are labeled as "Numerical Sol.," "Analytic Sol.," and "LeMessurier Sol.," in Fig. 17. For the numerical solution, the system critical load  $P_{cr}$  is calculated directly by the computer. Both the critical load  $P_{cr}$  and the effective length factor  $K$  of the strong shore can be found for the equation  $K = (P_e/P_{cr})^{0.5}$  where  $P_e$ =Euler critical load.

For the analytical solution, the slope-deflection method is used in the analysis. Four governing equations for models of A, B, C, and D are derived as follows:

$$\frac{S_{ij}^2}{S_{ii}} - S_{ii} + (m)k^2L^2 = 0 \quad (1)$$

( $m=1$  for model A,  $m=2$  for models B and C, and  $m=4$  for model D) where

$$S_{ii} = \frac{kL \sin kL - (kL)^2 \cos kL}{2 - 2 \cos kL - kL \sin kL}, \quad (2)$$

$$S_{ij} = \frac{(kL)^2 - (kL) \sin kL}{2 - 2 \cos kL - kL \sin kL}$$

and  $L$ =length of the column;  $k^2=P/EI$  ( $P$ =axial force,  $E$ =Young's modulus of the column; and  $I$ =moment of inertia of the column).

Based on the governing equation (1), the effective length factor  $K$  of the strong shore can be found. The critical load of the strong shore  $P_{cr}$  can be derived by the equation of  $K = (P_e/P_{cr})^{0.5}$ . Based on the critical load of the strong shore, the system critical load  $P_{cr}$  can be derived. Fig. 17 shows the analysis results of these three methods. The  $x$  axis expresses the analysis models, and the  $y$  axis is the system critical load.

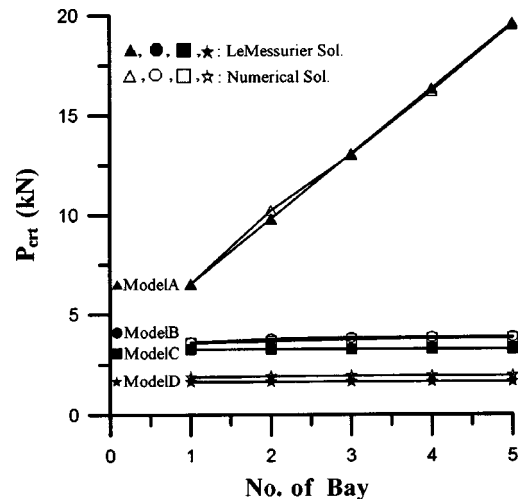


Fig. 18. System critical loads of numerical and LeMessurier formula solutions with different bays

For the leaning column effect, LeMessurier (1977) proposed the following formula to calculate the  $K$  factor:

$$K_i = \sqrt{\frac{\pi^2 EI}{L^2 P_i} \left( \frac{\sum P}{\sum P_{ek}} \right)} \quad (3)$$

where  $K_i$ =modified effective length factor of the column;  $P_i$ =axial force in the column;  $\sum P$ =axial loads on all columns in a story; and  $\sum P_{ek}$ =summation of the Euler buckling load of all columns in a story, which can be evaluated using the effective length obtained from monographs.

The analysis process using the LeMessurier formula is similar to the analytic solutions. The modified effective length factor of the strong shore is calculated by Eq. (3) first and the critical load of the strong shore is then determined. Finally, the system critical load is calculated.

As shown in Fig. 17, the numerical solution by the computer analysis and the analytic solution by the slope-deflection method are very similar. Except for model A, LeMessurier's solution generates smaller system critical loads than the other two methods. Basically, model A represents the upper strength bound of the systems, and it is not relevant and useful for design. Thus LeMessurier formula can be used to replace the complex numerical computer analysis in design.

For the 1-bay double-layer shoring system, the difference between the numerical and LeMessurier's solutions is small, say, less than 5% difference as shown in Fig. 17. The LeMessurier formula and analytical derivation are applicable in the analysis. The governing equation (1) can be easily solved by simple subroutines for solving nonlinear equations. After setting up of the governing equations, the critical loads can be found in a way similar to the LeMessurier formula. However, it is difficult to obtain the analytic solution for multibay shoring systems, which is a limitation of the method. Closed-form Eq. (1) is not available for multibay shoring systems.

#### Application of LeMessurier Formula in Multibay Systems

Based on the above discussion of the 1-bay case, the LeMessurier formula and numerical computer analyses for multibay shoring systems are compared. The LeMessurier formula in design is applied to models A, B, C, and D. Fig. 18 illustrates the system critical loads of the LeMessurier formula and the numerical com-



puter analysis for 1- to 5-bay systems. In the system, the heights of top and bottom shores are equal to the length of the horizontal stringer of 300 cm (9.8 ft). The solid symbols ( $\blacktriangle$ ,  $\bullet$ ,  $\blacksquare$ ,  $\star$ ) represent the results of the LeMessurier formula and the hollow symbols are calculated by computer. In Fig. 18, the curves obtained from the LeMessurier formula are very similar to the numerical solutions for models A, B, C, and D. This implies that the LeMessurier formula can replace the complicated numerical computer analysis in design, not only for 1-bay double-layer shoring systems, but also for multibay double-layer shoring systems.

Fig. 18 also shows that the system critical loads of model A increase linearly with the bay number of "strong shores." However, as the bay number of "leaning columns" increases, the system critical loads of models B, C, and D remain almost constant. Adding leaning columns in a double-layer shoring system does not increase system critical loads. Only adding strong shores is useful for increasing the system critical loads.

The above result is valuable for construction practice because failing to provide enough strong shores is very likely the main reason for system collapse. This point is easily overlooked since there exists a general impression that leaning columns help to increase the system critical load. This leads to collapse of falsework on a construction site and explains why small concrete loads can also cause shoring systems to collapse (see Fig. 3).

### Positions of Strong Shores

Based on the leaning column effect, the impact of different positions of strong shores which are installed on the top and bottom stories is investigated. The distances between shores and the stiffnesses of horizontal stringers are considered. The heights of bottom and top shores are both 300 cm (9.8 ft). A double-layer shoring system with a 5-bay model is used in the analysis.

Based on actual setup on the construction site, the spacing between shores in the shoring system is typically 60 cm (2 ft), i.e.,  $\beta=0.2$ . However, to allow for extreme conditions, the distance between shores is considered here. For such extreme case, a distance of 300 cm (9.8 ft) (i.e.,  $\beta=1.0$ ) is used. Additionally, horizontal stringers are always placed between the top and bottom shores as shown in Fig. 1. The stiffness of the stringer is relatively higher than an individual vertical shore since workers have a wrong impression that adding more stringers can make the system stable and safe. Again, to take into account the actual construction practice, the stiffness of the stringer is assumed 100 times of the stiffness of the shore in the analysis.

Fig. 19 shows the critical loads of the shoring systems against distances between shores and stiffnesses of stringers. Six cases for model D (see Fig. 4) with various positions of a strong shore on top and bottom stories are considered. Since the system is symmetrical without consideration of leaning columns and strong shores, only half of the system needs to be analyzed.

In Fig. 19, the strengths of double-layer shoring systems in cases 1 and 4, cases 2 and 5, and cases 3 and 6 are almost identical. This is because the heights of top and bottom shores are equal and the strong shores for the pair cases are simply imposed on the opposite positions. Thus cases 1, 2, and 3 can be respectively considered as equivalent to cases 4, 5, and 6 in this specific installation.

As shown in Fig. 19, when  $\beta$  is 0.2 and when the stiffness of the vertical shores  $E_h$  is the same as the horizontal stringer  $E_v$ , cases 1 and 4 have the lowest system critical load equal to 1,628 N (366 lb). However, the critical loads for cases 2 and 5 and cases 3 and 6 are about 1,765 N (397 lb). This phenomenon is also

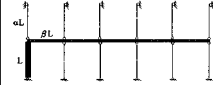



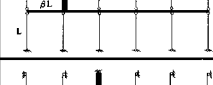
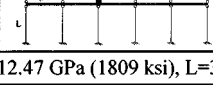
Cases		$P_{crit} (N)$		
		$\beta=0.2$	$\beta=1.0$	
No.	Positions of strong shore	$E_h=E_v$	$E_h=E_v$	$E_h=100E_v$
1		1628	1059	1952
2		1755	1344	1932
3		1765	1363	1932
4		1638	1059	1942
5		1755	1334	1932
6		1765	1363	1932
		$E_v=12.47 \text{ GPa (1809 ksi)}, L=300 \text{ cm (9.8 ft)}, \alpha=1$		

Fig. 19. Critical loads of double-layer shoring systems with various positions of a strong shore

noted in the model of  $\beta=1.0$ . The lowest value is 1,059 N (238 lb) for cases 1 and 4, which is lower than 1,334–1,363 N (300–306 lb) in cases 2 and 5 and cases 3 and 6. The system critical load for the model with  $\beta=0.2$  exceeds that for the model with  $\beta=1.0$  because the lengthening of the horizontal stringer reduces the end stiffness of the strong shore provided by the stringer. Fig. 12 demonstrates this relationship. Based on the analysis result, the system critical load is reduced by positioning the strong shore to the outermost location.

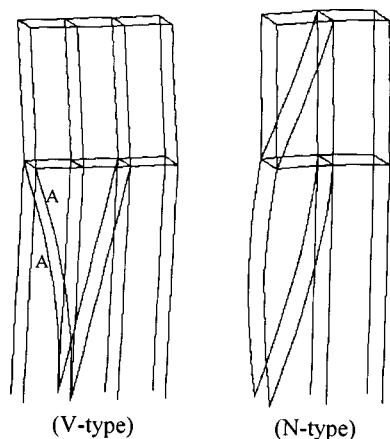
Fig. 19 shows that the critical loads of shoring systems almost do not change with the location of strong shores when a stiff horizontal stringer is used, i.e.,  $E_h=100E_v$ . Fig. 12 also shows this phenomenon. Since the horizontal stringer is stiff, the end stiffness provided by horizontal stringers is constant with respect to the  $P-\Delta$  effect, even though the strong shore is in different positions.

Based on the analysis results above, designers and workers should be reminded of the importance of the positions of strong shores when setting up double-layer shoring systems on the construction site. Strong shores in the outermost position are unfavorable for the system strength. Further, larger stiffness of the stringer leads to a higher system critical load.

### Strengthening of Double-Layer Shoring System

Theoretically, an appropriate lateral support at the position of the horizontal stringer prevents lateral deflection. However, this is not practical due to the constraints on construction sites. The concept of strong shores can be well accepted in construction practice. This paper proposes reinforcement to the shoring system based on the equivalent strong shores. Installed slant braces in the system transfer horizontal forces to the ground, which improves the strength of the system. Two simple setups of the slant braces are proposed in Fig. 20.





**Fig. 20.** Double-layer shoring system with V-type and N-type bracings after loading

### Reinforcement by V-Type Bracing

In Fig. 20, the slant braces on the bottom story of shape V in the left picture are defined as the V-type reinforcement in this paper. In the shoring system, the equivalent strong shore with six vertical shores and four slant braces is considered as an equivalent strong shore in a closed-form style. The dimensions of the shoring systems in Fig. 20 are 300 cm (9.8 ft) ( $L$ ) for the height of bottom shores, the height of the top shores is 180 cm (5.9 ft) ( $\alpha=0.6$ ), and the spacing between the shores is 60 cm (2 ft) ( $\beta=0.2$ ). (Refer to Fig. 6 for details). This setup is appropriate for testing (see Fig. 9). All the elastic moduli of vertical shores and horizontal stringers are the same as the last examples.

The analysis model in Fig. 20 is a three-dimensional model. Only the direction perpendicular to the horizontal stringers, i.e., out of the paper, is restrained. The end nodes of each shore are assumed as hinged supports, and the stringer is a continuous prismatic member. Except for the ten shores used as an equivalent strong shore, the shores can be considered as leaning columns. All these assumptions are selected to model the test setup by Peng et al. (1998).

The diagram on the left in Fig. 20 shows the deformed shape of the structure after loading. There is little lateral deflection at the horizontal stringer when compared with Fig. 10(a). The main deformation is located at the left slant braces labeled "A" in the left picture in Fig. 20. The slant braces provide an extremely good sidesway restraint in the system. The critical load of the shoring system is calculated as 178,487 N (40,124 lb). This value is much higher than the critical load of 2,452 N (551 lb) for the 2-bay system without the brace reinforcement in Fig. 8. The V-type reinforcement can provide a very good stiffening system to the double-layer shoring system.

### Reinforcement by N-Type Bracing

Another reinforcement is shown in the right picture in Fig. 20. Slant braces are installed on top and on bottom stories. This installation, in the form of a deformed leaning letter N, is defined as N-type reinforcement. The shores with these slant braces in the system can be considered as two equivalent strong shores on top and on bottom stories. In this system, all the assumptions of dimensions, boundary conditions, elastic modulus, and end nodes of members are the same as the V-type reinforcement. All shores except for the equivalent strong shores can be considered as leaning columns (i.e., the four columns on the right-hand side).

As shown in Fig. 20, the picture on the right-hand side is the system deformation with N-type bracing after loading. In this figure, the lateral deflection of the horizontal stringer is not apparent. The primary deformation in the system is on the shores and slant braces of the equivalent strong shore in the bottom story. Since the vertical shores in the equivalent strong shore of the N-type are less than the V-type, the deformation of N-type is larger than V-type.

For the N-type bracing case, the critical load of the shoring system is 61,784 N (13,889 lb). The value is also higher than the critical load of 2,452 N (551 lb) for the 2-bay model in Fig. 8. The reinforcement of N-type is not as strong as the V-type since their failure modes are different. However, both systems can provide a load-carrying capacity in a double-layer shoring system that exceeds the construction load.

For these two reinforcement models, if only the bottom story is considered, the approximate load capacity of each shore is 14,874 N (3,344 lb) ( $=178,487/12$ ) for V-type and 7,723 N (1,736 lb) ( $=61,784/8$ ) for N-type. The load capacity for V-type reinforcement is twice that of the N-type reinforcement (i.e.,  $14,874/7,723=1.93$ ).

### Conclusions

The paper studies the buckling capacities of double-layer shoring systems by numerical analyses supported by some tests. The following conclusions can be drawn.

1. Adding strong shores is an effective method to increase the system critical load. Increasing the number of leaning columns does not help to improve the system strength of the falsework. However, strong shores and leaning columns can hardly be distinguished by workers; this situation leads to a potential danger on construction sites.
2. The results of 2D and 3D analyses are fairly similar for the specified installation. Thus a 2D analysis can be used to replace the more complicated 3D analysis in these particular cases.
3. Model D with three leaning columns represents the worst setup of double-layer shoring systems on a construction site according to test results in Taiwan. Additionally, real system critical loads should be located between model D and model A with four strong shores, based on the usage of strong shores and leaning columns.
4. When the stiffness of the horizontal stringer decreases, the system critical load also reduces for an unsymmetrical arrangement of strong shores to the line of the horizontal stringer in models C and D.
5. For an unsymmetrical arrangement of strong shores in models C and D, the system critical load increases with a decrease in length of the horizontal stringer.
6. For simplicity, the analytical and the LeMessurier formula can be used to replace the complicated numerical analysis for the 1-bay system. The LeMessurier formula is also applicable to other multibay systems in design.
7. Strong shores on the outmost location are not effective in increasing the system critical load.
8. When the height of the bottom shores is constant with the increased length of top shores, the system critical loads of models A and B are much higher than models C and D. The shorter the length for top shores, the bigger discrepancy between the two conditions.
9. As reinforcement to a double-layer shoring system, V-type and N-type models are helpful in strengthening the system

confirmed by rigorous second-order analyses. Each shore on the bottom story in the V-type model provides about twice the strength of the N-type model.

## Acknowledgments

The writer acknowledges Professor S. L. Chan of the Hong Kong Polytechnic University and Professor W. F. Chen of the University of Hawaii for their invaluable comments. The writer also thanks graduate students C. H. Kung and W. C. Huang for their help in performing the tests. The financial support of the National Science Council (NSC88-2211-E-324-004), Taipei, Taiwan is greatly appreciated.

## References

- Chan, S. L., and Zhou, Z. H. (1994). "A pointwise equilibrium polynomial (PEP) element for nonlinear analysis of frame." *J. Struct. Eng.*, 120(6), 1703–1717.
- Council of Labor Affairs. (1997). "Investigations of construction accidents: 1993~1995." (*IOSH86-03*), *Research Rep.*, Taipei, Taiwan (in Chinese).
- El-Shahhat, A. M., Rosowsky, D. V., and Chen, W. F. (1994). "Construction safety of multistory concrete buildings." *ACI Struct. J.*, 91(4), 475–485.
- LeMessurier, W. J. (1977). "A practical method of second order analysis, Part 2—Rigid frames." *AISC Eng. J.*, 14(2), 49–67.
- Mosallam, K., and Chen, W. F. (1990). "Design considerations for formwork in multistory concrete buildings." *Eng. Struct.*, 12(7), 163–172.
- Peng, J. L. (2002). "Stability analyses and design recommendations for practical shoring systems during construction." *J. Constr. Eng. Manage.*, 128(6), 536–544.
- Peng, J. L., Kung, C. H., and Huang, W. C. (1998). "Load-carrying capacity of double-layer falsework systems." *Structural Engineering Rep.*, Chaoyang University of Technology, Taichung, Taiwan (in Chinese).
- Peng, J. L., Pan, A. D., Rosowsky, D. V., Chen, W. F., Yen, T., and Chan, S. L. (1996a). "High clearance scaffold systems during construction, Part I: Structural modeling and modes of failure." *Eng. Struct.*, 18(3), 247–257.
- Peng, J. L., Rosowsky, D. V., Pan, A. D., Chen, W. F., Chan, S. L., and Yen, T. (1996b). "High clearance scaffold systems during construction, Part II: Structural analysis and development of design guidelines." *Eng. Struct.*, 18(3), 258–267.
- Peng, J. L., Yen, T., Lin, I., Wu, K. L., and Chen, W. F. (1997). "Performance of scaffold frame shoring under pattern loads and load paths." *J. Constr. Eng. Manage.*, 123(2), 138–145.